Synthesis and investigation of magnetic and transport properties of $La_{0.5}Sr_{0.5}MnO_3$ nanostructured material

David Scott

LASiGMA SUBR REU participant.

Home institution, Norfolk State University; Norfolk, VA 23504

Abstract

Bulk $La_{0.5}Sr_{0.5}MnO_3$ was synthesized using a solid state reaction method. X-Ray diffraction was used to confirm the composition of the material. Some interesting electrical and magnetic properties were observed after the material was prepared.

1. Introduction

Looking at today's world from a technological view, it is changing rapidly. There is an ongoing race to develop faster, smaller and more efficient computing capabilities. These capabilities rest upon the materials they are made from. As better materials are developed, the industry progresses.

This project's goal was to synthesize $La_{0.5}Sr_{0.5}MnO_3$ with grain size in the nm range. Although this material is ceramic, it displays some very interesting electrical and magnetic properties. These make it potentially useful in the area of computing materials applications.

2. Background

This section gives a brief discussion in order to familiarize the reader about the methods used in the experimentation. Solid state synthesis, x-ray diffraction and resistivity will be discussed.

2.1 Solid State Reactions

A solid State Reaction, also known as a dry-media reaction or a solventless reaction, is a chemical reaction that does not involve a solvent. Often times chemical reactions require the compounds to be placed in a solvent before a reaction can take

Figure 1 Reactants being mixed together ($2La_2O_3 + 4SrCO_3 + 8MnO_2$)

place; solid state reactions do not require such. The solids are brought together and thoroughly mixed. After they are mixed it is sometimes necessary to heat the mixture to encourage the reaction to take place. The heating of the material adds energy to the system. The added energy increases the kinetic energy of the constituent atoms resulting in the desired reaction. Solid state synthesis can be advantageous because of the simple fact that it does not require a solvent. The exclusion of a solvent is an advantage because it reduces material expenses. Also, the solid state synthesis eliminates unwanted by-products which may also raise issues of contamination and disposal.

2.2 X-Ray Diffraction

X-ray diffraction is a very useful tool for obtaining structural and identification information about a material sample. X-ray diffraction is useful in the characterization of crystalline material. In x-ray diffraction procedure, electrons are emitted from a filament and strike a target. Collisions with the target produce x-rays which are then allowed to strike the sample. Reflections from the atomic planes in the sample are collected by a detector. The output of the detector from the x-ray diffractogram gives the picture or data. Depending on the material of the sample, the x-rays will deflect at specific angles, resulting in characteristic intensity peaks.

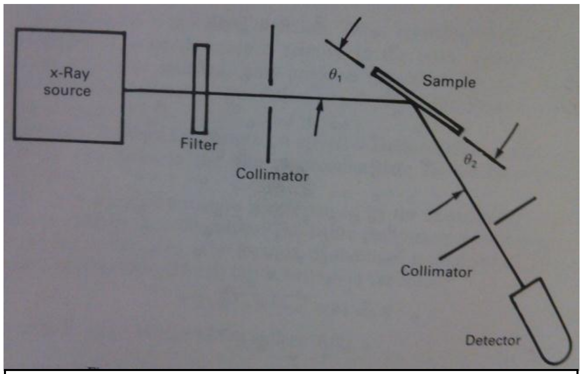

Figure 2 This diagram is a simple sketch of an XRD machine.

The pattern of the intensity peaks vs. the angle of reflection is unique to the specific crystal structure and composition of the sample. The arrangement of the atoms varies from material to material. There are a number of structures in which the atoms arrange themselves i.e., the crystal structure. The arrangement of the atoms determines the reflection of the x-rays. See figure 2.

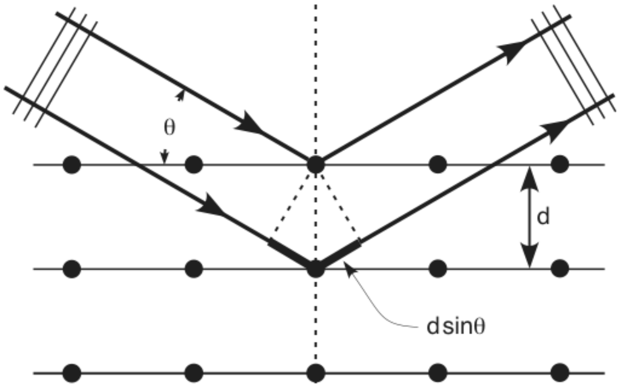

Figure 3 The Scattering of X-Rays from crystal Planes

Because each material is composed of different atoms, which make different structures, the reflection of x-rays from every material will be unique. The intensity of the reflections are measured and graphed; the graph is usually referred to as a diffractogram. A common label for the axes of the diffractogram is intensity, along the vertical axis, and two-theta degrees along the horizontal axis.

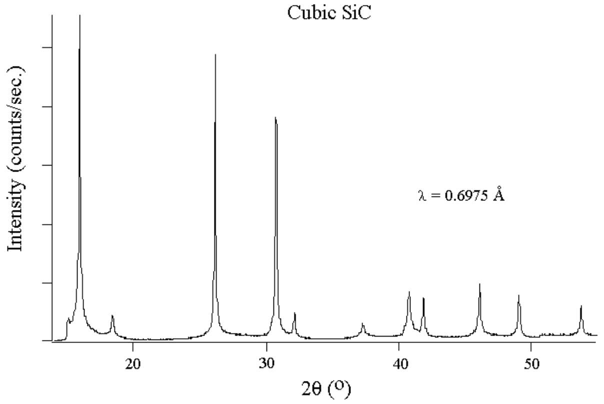

[D]Figure 4 Experimental x-ray diffraction patterns of cubic SiC using synchrotron radiation

Figure 3 shows a specific example of an x-ray diffractogram. This x-ray diffractogram is the "fingerprint" of cubic SiC. By comparing the locations of the intensity peaks to accepted data, a determination, of whether SiC is present, can be made. This is one process by which chemical composition can be obtained. Each element and chemical compound has its own unique "fingerprint." The x-ray data of a compound will show various intensity peaks. The peaks will be at specific locations depending on which elements are in the compound. Software has been developed to simplify this process enormously. Some software analyzes the peaks; and based on the positions and intensities of the peaks, generates a list of best matches for the chemical composition. The documented XRD results from the software's database can be superimposed onto the experimental results and a comparison of the two x-rays can be conducted.

2.3 Resistivity

Resistivity is the opposition to an electric current and is an intrinsic property of the material. It is directly proportional to resistance. They are related through the following equation:

$\rho = \frac{RA}{l}$, where ρ= resistivity (Ω-cm), A = cross sectional area (cm^2) and ℓ = length (cm).

Resistance is caused by electron collisions. In a material, you have numerous electrons occupying space. Applying an electric current to a material forces electrons to travel through the material. The structure of the material determines how easily the electrons will move. The resistance depends on the geometry or shape of the sample.

3. Method

This section discusses the synthesis of both sample #062011 and sample #062911.

3.1 Synthesis of Sample #062011

The goal, for sample #062011, was to make 2 grams of $La_{0.5}Sr_{0.5}MnO_3$. The starting compounds were lanthanum (III) oxide (Alfa Aesur 99.999% purity), strontium carbonate (Alfa Aesur 99.999% purity) and manganese (IV) oxide (Alfa Aesur 99.999% purity).

The balanced chemical equation to obtain the desired compound is:

$2La_2O_3 + 4SrCO_3 + 8MnO_2 \rightarrow 8\ La_{0.5}Sr_{0.5}MnO_3 + 4CO_2 + O_2$

After the equation was balanced, stoichiometric calculations were performed in order to determine the amount of each reactant that is needed to produce the desired amount of product. In the following calculations the desired product, $La_{0.5}Sr_{0.5}MnO_3$, is referred to as P_x .

For La_2O_3:

$$2g\ P_x \times \frac{1\ mol\ P_x}{216.3\ g} \times \frac{2\ mol\ La_2O_3}{8\ mol\ P_x} \times \frac{326\ g}{1\ mol\ La_2O_3} = \frac{1304}{1730.4} = 0.7536\ g$$

For $SrCO_3$:

$$2g\ P_x \times \frac{1\ mol\ P_x}{216.3\ g} \times \frac{4\ mol\ SrCO_3}{8\ mol\ P_x} \times \frac{147.6\ g}{1\ mol\ SrCO_3} = \frac{1180.8}{1730.4} = 0.6824\ g$$

For MnO_2:

$$2g\ P_x \times \frac{1\ mol\ P_x}{216.3\ g} \times \frac{8\ mol\ MnO_2}{8\ mol\ P_x} \times \frac{87\ g}{1\ mol\ MnO_2} = \frac{174}{216.3} = 0.8044\ g$$

After obtaining the appropriate quantity of each starting compound, the sample fabrication process was begun.

In order to ensure that enough of the starting compounds remain after mixing (there may be some spillage or other means of loss of sample) the amount of each of the starting compounds was increased by 0.05 g

Based on the above calculations, 0.8 g of La_2O_3, 0.72 g of $SrCO_3$ and 0.85 g of MnO_2 was measured using a laboratory balance. These were mixed together in an agate mortar and ground, manually, for approximately thirty minutes. The color of the resulting powder was a grayish black and the texture was a fine uniform powder.

After grinding, the powder was placed in an alumina, boat shaped crucible. As seen in the balanced equation, in addition to the $La_{0.5}Sr_{0.5}MnO_3$ we also have $4CO_2$ and O_2 as by-products. One way to eliminate these unwanted by-products is by heating the mixture at high enough temperatures that the unwanted compounds will be released. This process is called decarbonization. So, decarbonization simply means to remove the carbon from the desired result. Based on previous experience, heating the sample at temperatures above 1100°C is sufficient to release the unwanted CO_2 and O_2.

To carry out the decarbonization process, the ceramic crucible containing the mixed powder was placed at the center of a tubular furnace. The furnace was then programmed to ramp the temperature at the sample from room temperature to 1150°C at a rate of 5°C per minute. Then this temperature at the sample was held constant for 12 hours. After the 12 hours the furnace was programmed to cool to room temperature at a rate of 5°C per minute. The heating was done in air. Figure 5 shows a representation of the decarbonization heating profile.

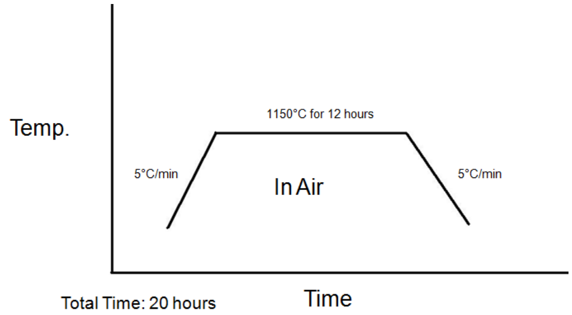

Figure 5 Decarbonization heating profile for high temperature furnace.

Following the decarbonization process, x-ray diffraction data of a portion of the powder sample were collected to check for the presence of carbon.

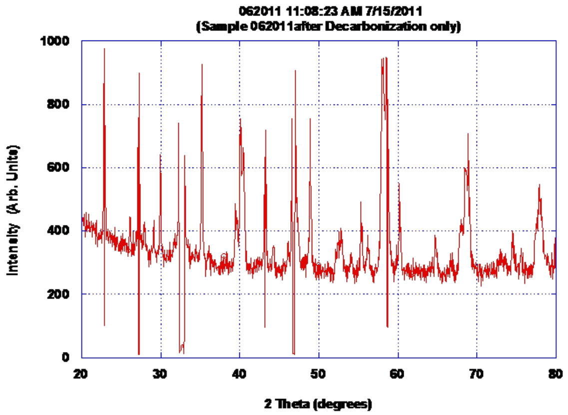

Figure 6 X-ray diffractogram for sample #062011 following the decarbonization process.

The other part of the sample was first reground using the agate mortar and pestle and then pressed into a pellet using a hardened stainless steel die in a hydraulic press. The pellet was a small circular shape disk with a width of approximately 3 mm and a diameter of about 15 mm, with a mass of 0.512 g.

The sample was pressed into a pellet to get the powder grains into as close in proximity as possible so that under further processing (sintering) the desired reaction to produce the product will be enabled. After the pellet was pressed, it was placed into an alumina crucible which was then returned to the high temperature furnace for the sintering process.

Sintering is a process by which the sample is heated at high enough temperatures long enough to permit the desired reaction to take place. During the process, the heat energy that is applied causes the atoms in the material to gain enough kinetic energy to enable the desired reaction. It is important that the heating does not exceed the melting point of the sample but is enough to cause the desired reaction. The sintering profile is given below:

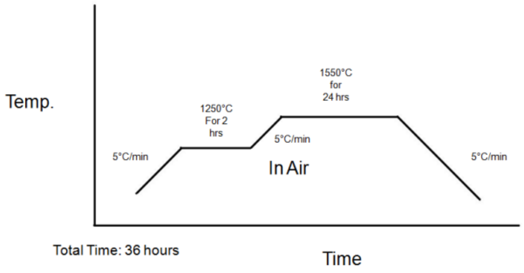

Figure 7 Sintering profile for sample #062011

The furnace was programmed to heat the sample from room temperature to 1250°C at 5°C per minute, then remain constant (dwell) at 1250°C for 2 hours. Next, the temperature should rise to 1550°C at 5°C per minute and dwell at 1550°C for 24 hours. Following the 24 hours, the furnace would cool at 5°C per minute back to room temperature. Figure 7 is the temperature profile for the sintering process.

3.2 Synthesis of Sample #062911

The goal for sample #062911 was to produce 5 grams of $La_{0.5}Sr_{0.5}MnO_3$. The starting compounds were lanthanum (III) oxide (Alfa Aesur 99.999% purity), strontium carbonate (Alfa Aesur 99.999% purity) and manganese (IV) oxide (Alfa

Aesur 99.999% purity). Because the quantity we are seeking changed, more stoichiometric calculations needed to be performed to obtain the correct amout of reactants. The calculations are below:

For La_2O_3:

$$5g\ P_x \times \frac{1\ mol\ P_x}{216.3\ g} \times \frac{2\ mol\ La_2O_3}{8\ mol\ P_x} \times \frac{326\ g}{1\ mol\ La_2O_3} = \frac{3260}{1730.4} = 1.884\ g$$

For $SrCO_3$:

$$5g\ P_x \times \frac{1\ mol\ P_x}{216.3\ g} \times \frac{4\ mol\ SrCO_3}{8\ mol\ P_x} \times \frac{147.6\ g}{1\ mol\ SrCO_3} = \frac{2952}{1730.4} = 1.706\ g$$

For MnO_2:

$$5g\ P_x \times \frac{1\ mol\ P_x}{216.3\ g} \times \frac{8\ mol\ MnO_2}{8\ mol\ P_x} \times \frac{87\ g}{1\ mol\ MnO_2} = \frac{435}{216.3} = 2.011\ g$$

As we did before, we added 0.05 g to the calculated quantities. So we measured out 1.934 g of La_2O_3, 1.757 g of $SrCO_3$ and 2.061 g of MnO_2. These were mixed in the agate mortar and ground together, manually, for approximately thirty minutes. The color was of the mixture was a grayish black and the texture was a fine uniform powder. Next decarbonization was carried out.

A total of 5.010 g of sample was loaded into the furnace for decarbonization. We programmed the furnace to raise the temperature to 1150°C at a rate of 5°C per minute and heat the sample for 12 hours in air. After the 12 hours the furnace was programmed to cool at a rate of 5°C per minute.

Following decarbonization, the sample was pressed into two pellets. The remaining sample that was not used was stored in a vial. The pellets, with a combined mass of 2.742 g, were then sintered in the furnace.

The furnace was then programmed to rise from room temperature to 1562°C at a rate of 12°C per minute. It would dwell at 1562°C for 20 hours then it would cool down to room temperature at a rate of 12°C per minute. Figure 8 is a profile of the sintering process.

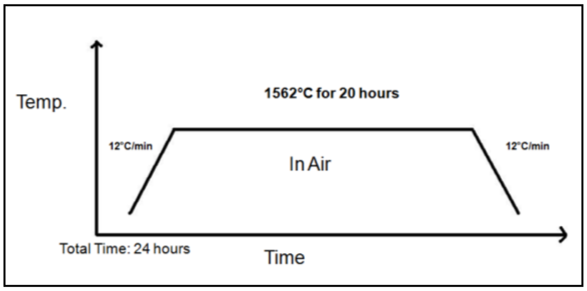

Figure 8 Heating profile for Sintering of sample #062911

The only differences between sample #062011 and sample #062911 are the amounts of sample that was prepared and the sintering processes. Only 2 grams of sample #062011 was prepared versus the 5 grams of sample #062911. The sintering process for sample #062011 consisted of two dwelling periods, the first at 1250°C for 2 hours and the second at 1550°C for 24 hours. Sample #062911only had one dwelling period which was at 1562°C for 20 hours.

4. Results & Discussion

Both of the samples show the same composition. Hence, the discussion that follows will focus on only the 062911 sample since the data should be similar for the other sample.

This section discusses analysis of the experimental results. It includes an examination of the XRD data for the #062911 sample, a discussion of the crystallite size, a discussion of the resistivity and the magnetization of the sample of the sample.

4.1 XRD Results

After preparing the sample, it is necessary to verify the chemical composition. Without this step, there is no concrete evidence that tells us that we ended up with the product that we were trying to obtain. Composition determination was done via x-ray diffraction. As was explained before, the x-ray diffraction data shows what elements are in the sample.

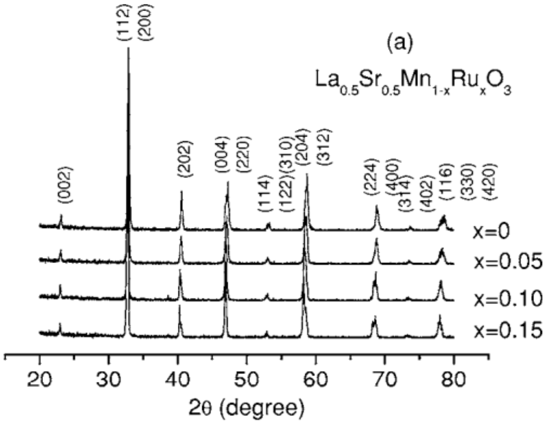

[E]Figure 9 X-ray diffraction pattern of $La_{0.5}Sr_{0.5}Mn_{1-x}Ru_xO_3$

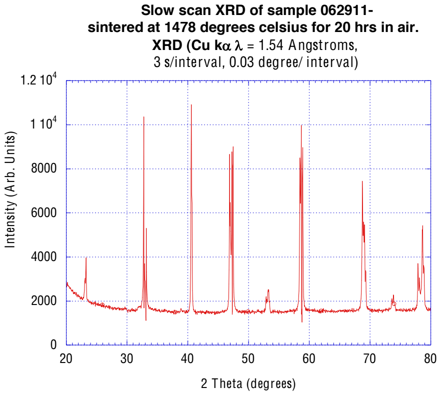

Figure 10 X-ray diffraction pattern for sample #062911 after sintering

Figure 9 is x-ray diffraction data for $La_{0.5}Sr_{0.5}Mn_{1-x}Ru_xO_3$, which when x = 0 gives a compound that is the same as what our desired composition is. Consequently, if we compare the x-ray diffraction data from our samples with that in Fig. 9, then the x-ray data from our samples should correspond to the x-ray data for $La_{0.5}Sr_{0.5}Mn_{1-x}Ru_xO_3$ when x=0. Inspection of figures 9 and 10 show an excellent match between the two sets of data (x = 0 in figure 9 and figure 10) with respect to the intensity peaks vs.2θ degrees.

Peak Position $La_{0.5}Sr_{0.5}Mn_{1-x}Ru_xO_3$ For x=0	Peak Position Sintered Sample #062911	% Difference	Crystal Size
23	23.3	1.29	
32.5	32.9	1.22	119
40.6	40.8	0.49	103
46.9	47.4	1.06	97.54
52.6	53.3	1.32	
58.2	58.7	0.85	144.5
68.5	68.7	0.29	126.5
73.7	73.7	0	
78.7	78.7	0	

Table 1 Peak position comparison and Crystallite Size Calculations

In table 1, we have carefully calculated the location of each peak from both sets of data (x = 0 in figure 9 and figure 10). The two sets of peaks match within 2% of one another.

4.2 Crystallite Size

Table 1 also shows the estimated crystallite sizes for our bulk sample #062911. Crystallite size estimation was based on using the #062911diffractogram data and Scherrer's equation.

$$\tau = \frac{K\lambda}{\beta \cos\theta}.$$

τ is the mean size of the crystallites, which may be smaller or equal to the grain size, λ=1.54 Angstroms is the x-ray wavelength of the k_α radiation of the copper x-ray target, K is the shape factor, usually 0.9, β is the full-width of the peak at half the maximum intensity (FWHM) in radians and θ is the angle where the peak is located. Scherrer's equation gives a lower bound of the particle size. If the diffractogram's peak solely depended on crystallite size, then the equation would give a fairly accurate account of the crystallite size. In order to obtain an estimate of the crystallite size the diffraction peak is fitted to a guassian curve.

$$y = m_1 + m_2 e^{[\frac{(m_3 - m_0)}{m_4}]^2} ,$$

Where Y represents the intensity of the peak, m_1 is the value that the bottom of the curve approaches, m_2 is the maximum value of the peak, m_3 is the value of the middle of the peak in terms of 2θ and m_4 is a number between zero and one.

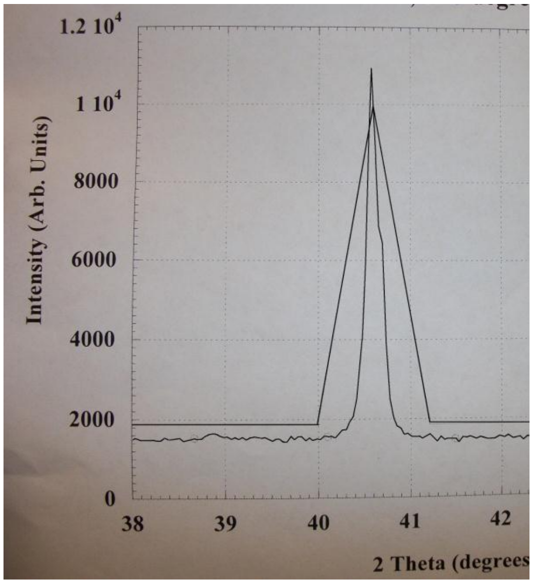

Figure 11 A bell curve being fixed to peak in the diffractogram.

As can be seen in figure 11, the curve fit is more triangular as opposed to a typical bell shaped guassian curve. This will introduce some error into our estimates.

Next is an example of how Scherrer's equation was used to calculate the crystallite size.

Using the intensity peak at 2Theta = 40.62 degrees, and K= 0.9,

β = 0.86° = 0.015 radians,

λ = 1.54 Angstroms,

With θ = 20.31 degrees

The crystallite size is estimated to be

$$\tau = \frac{K\lambda}{\beta \cos\theta} = \frac{(0.9)(1.54\ \acute{A})}{(0.015\ rad)\cos(20.31)} = 103\ \dot{A}$$

Estimates of the crystallite sizes are given in table 1. Taking an average of the estimates we can see that our crystallite size is of the order of 10 nm.

4.3 Resistivity

We also investigated the resistivity of our sample. Using a small piece of our sample #062911 (see the center of figure 14), the resistance was measured using a four-probe method. Four wires were connected to the sample, as illustrated in figure 12, using silver paste. A four probe resistance measuring device (Keithley 2010 multimeter) was used to determine the resistance. Figure 13 shows a sketch of the four probe method that was used to find the resistivity.

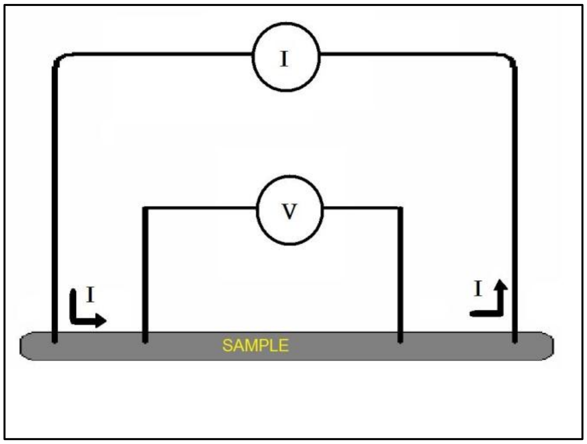

Figure 12 An illustration of the four probe method

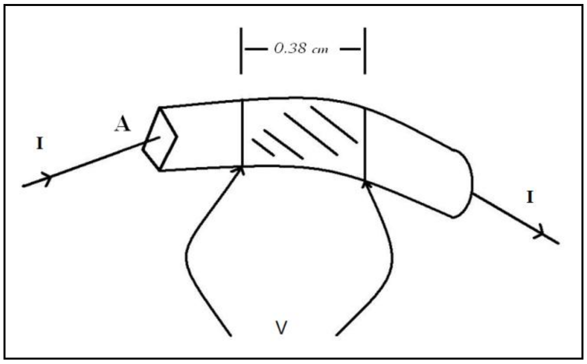

Figure 13 Sketch of four probe method on the sample

The voltmeter gave a resistance value of 0.11 Ω for the sample. By using the resistance and the dimensions of the samples we can calculate the sample's resistivity using the following equation:

$\rho = \frac{RA}{l}$, where ρ= Resistivity, A = cross sectional area and l= length

$$\rho = \frac{RA}{l} = \frac{(0.11\ \Omega)(0.011\ cm^2)}{(0.38\ cm)}$$

$$= \frac{0.0021\ \Omega{\cdot}m}{0.38} = 3.18E^{-3}\ \Omega \cdot m,$$

Or $\rho = 3.18 \times 10^{-1}\ \Omega$-cm.

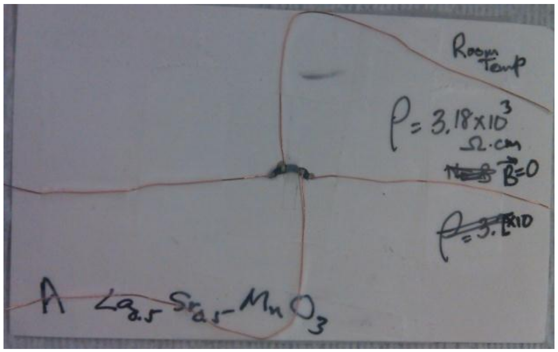

Figure 14 Four leads were attached to the sample with silver paint employing the 4-probe method.

4.4 Physical characteristics

Following the sintering, the sample was examined. The pellet that was placed in the boat was no longer intact. It had collapsed into pieces. There was one larger piece and the rest was in smaller pieces. The sample was a dark grayish color. It seemed hard but also brittle. The sample also possessed some metallic properties as seen by the very low resistance (low resistivity as seen above) when it was measured with a multimeter. It also displayed paramagnetic behavior i.e. it was attracted to the poles of a permanent magnet.

The odd thing about the substance displaying metallic properties is that the substance is a ceramic material! It is fairly well known that ceramics are not good conductors at all. In fact, ceramics are largely considered to be insulators. This being the case, the fact that the voltmeter was showing little to no resistance is quite bizarre. Apparently, this ceramic material is acting as a very good conductor which is very uncharacteristic.

The other new property that was mentioned was the paramagnetism. This phenomenon was especially intriguing. The starting compounds, La_2O_3, $SrCO_3$ and MnO_2, display no magnetic properties (i.e., they are not attracted to a permanent magnet). However, upon the decarbonization and sintering of our product, $La_{0.5}Sr_{0.5}MnO_3$, some magnetic properties were acquired. Paramagnetism means that the sample is attracted to the magnetic field of the magnet but in absence of the magnet, it did not display magnetic properties neither did it retain any of the magnetism after the magnet was removed.

5. Conclusion

This project is laying the foundation for a continuing research project. The main goal of the project was to develop a successful synthesis method that produces bulk $La_{0.5}Sr_{0.5}MnO_3$ with nanostructures. This was accomplished.

Future work for this project includes the development of a suitable method to produce high quality $La_{0.5}Sr_{0.5}MnO_3$ and other half-metallic, rare earth-transition metal oxide nanoparticles and nanostructured materials. The mentor plans to continue the project to investigate and modify the magnetic and charge transport properties of some half-metallic rare earth transition metal oxide nanoparticles.

6. Acknowledgements

Support for the summer research project was from the LA-SiGMA REU Program, funded by the National Science Foundation, through the Department of Physics at Southern University and A&M College. Thanks to Scott Wicker and Dr. E. Walker for help with the XRD component and Dr. Laurence L. Henry who was my mentor for the project.

---

7. References

A. "Basics of X-Ray Diffraction." Scintag, Inc, 1999. Web. 13 July 2011. <http://epswww.unm.edu/xrd/xrdbasics.pdf>.

B. Anglin, M. R. "What Is a Solid State Reaction?" *WiseGEEK: Clear Answers for Common Questions*. Conjecture Corporation, 9 June 2011. Web. 13 July 2011. <http://www.wisegeek.com/what-is-a-solid-state-reaction.htm>.

C. P. Scherrer, "Bestimmung der Grösse und der inneren Struktur von Kolloidteilchen mittels Röntgenstrahlen," *Nachr. Ges. Wiss. Göttingen* 26 (1918) pp 98-100.

D. Schields, Paul J. "Bragg's Law and Diffraction." *Earth Science Educational Resource Center*. Web. 13 July 2011. <http://www.eserc.stonybrook.edu/ProjectJava/Bragg/>.

E. Ying, Yue, Jiyu Fan, Li Pi, Zhe Qu, Wenqin Wang, Bo Hong, Shun Tan, and Yuheng Zhang. "Effect of Ru Doping in $La_{0.5}Sr_{0.5}MnO_3$ and $La_{0.45}Sr_{0.55}MnO_3$." *Physical Review B* 74.14 (2006). Print.